BE ANALYSIS OF BOTTOM SEDIMENTS IN DYNAMIC FLUID-STRUCTURE INTERACTION PROBLEMS

J. J. AZNÁREZ [1], O. MAESO [1] AND J. DOMÍNGUEZ [2] [*]

[1]   Instituto Universitario de Sistemas Inteligentes y Aplicaciones Numéricas en Ingeniería (IUSIANI), Universidad de Las Palmas de Gran Canaria, Campus Universitario de Tafira, 35017, Las Palmas de Gran Canaria, Spain.

[2]   Escuela Superior de Ingenieros, Universidad de Sevilla, Camino de los Descubrimientos s/n, 41092, Sevilla, Spain. E-mail: jose@us.es

[*]Corresponding author

SUMMARY

Sediment materials play an important role on the dynamic response of large structures where fluid-soil-structure interaction is relevant and materials of that kind are present. Dam-reservoir systems and harbor structures are examples of civil engineering constructions where those effects are significant. In those cases the dynamic response is determined by hydrodynamic water pressure, which depends on the absorption effects of bottom sediments. Sediments of very different mechanical properties may exist on the bottom.

A three-dimensional BE model for the analysis of sediment effects on dynamic response of those structures is presented in this paper. One of the most extended models for sediment materials corresponds to Biot's fluid-filled poroelastic solid. The BE formulation for dynamics of poroelastic solids is reviewed including a weighted residual formulation more general and concise than those previously existing in literature. Systems consisting of water, other pressure wave propagating materials, viscoelastic solids and fluid-filled poroelastic zones, are studied. Coupling conditions at interfaces are taken into account in a rigorous way. A simple geometry coupled problem is first studied to asses the effects of sediments on its dynamic response and to determine the influence of parameters such as sediment depth, consolidation, compressibility and permeability. A fully 3-D arch dam-reservoir-foundation system where sediments and radiation damping play an important role is also studied in this paper. Obtained results show the importance of a realistic representation of sediments and the influence of their consolidation degree, compressibility and permeability on the system dynamic response.

KEY WORDS: Porous saturated solids; dynamic response; fluid-structure interaction; bottom sediments; wave propagation; boundary element method.

INTRODUCTION

This paper is intended to present a three-dimensional boundary element (BE) model and its application to the dynamic analysis of coupled structural systems including different kind of regions: solids, fluids, and fluid saturated porous materials. The model is used to study the influence of sediment materials and their properties, on the dynamic response of large civil engineering structures such as dams and harbor structures which are examples of constructions where those effects are significant.

In the case of seismic behavior of concrete dam-reservoir systems, factors related to hydrodynamic pressure on the dam upstream face are particularly important. Bottom sediments absorb energy of the hydrodynamic waves and therefore increase damping in the dam-reservoir-foundation system. Due to gravity, sediments may acquire a certain level of gradual consolidation through depth during the sedimentation process. Thus, the sediment is a material whose properties vary with depth and are different to those of the reservoir water. Sediments with a high level of consolidation provide the system with a significant energy dissipation capacity and can be modelled as a porous saturated material. In the present study, the concrete dam will be represented as a viscoelastic solid, the water as an inviscid compressible fluid, and the sediment, depending of its consolidation degree, as a compressible scalar domain with depth increasing density, as a porous saturated medium whose skeleton has acquire certain elastic capacity, or as a combination of both.

Numerous studies related to dam-reservoir systems where bottom sediments are represented as viscoelastic solids [1-4] o poroelastic domains [4-11], have been published in the literature. Porous sediment effects on hydrodynamic pressure were first

analyzed by Cheng [5] who showed the influence of their compressibility, highly dependent on the presence of undissolvable gases, using a one dimensional model. Bougacha and Tassoulas [6-8], Chen and Hung [9] and Domínguez et al. [10] studied the effects of sediments on gravity dam response using coupled 2-D models where the sediment is a Biot´s poroelastic material and water-sediment and foundation-sediment interaction are considered using 2-D equilibrium and compatibility conditions. Those authors concluded that bottom sediments can change the dynamic behavior of the system to a significant extent, in particular when the sediments are partially saturated.

To the best of our knowledge, the only model existing in the literature dealing with the dam-reservoir-sediment system as a fully coupled 3-D dynamic system is that recently presented by the authors [11]. This three-dimensional model was developed for the analysis of porous material effects on dynamic response of arch dams, harbor structures and other fluid-structure mechanical systems containing porous domains. It is based on previous 3-D Boundary Element models developed by the authors for the seismic study of arch dams including water-soil-structure interaction effects [12,13], and on a 2-D model presented in [10] for the analysis of porous sediment effects on gravity dams. All the regions in the system; i.e., viscoelastic solids, compressible fluids and two-phase fluid saturated porous materials, which behavior is described by Biot´s theory [14], are represented by boundary integral equations and discretized into boundary elements. The boundary integral equations for dynamic behavior of porous materials were first presented by Domínguez [15,16] and by Cheng et al. [17], in slightly different form. The formulation presented in the present paper starts from weighted residual statements in terms of only four variables and is simplified by the use of equivalent complex densities including dissipation. The resulting integral equations are equivalent to those

in refs. [10,15-17]. Interaction between different materials is accounted for rigorously by setting equilibrium and compatibility conditions on interfaces. The analysis is carried out in the frequency domain.

The main objectives of the present study are: first, to improve a coupled 3-D boundary element model able to properly represent all the regions of the problem and the important dynamic interaction phenomena existing between them; second, to analyze the effects that bottom sediments with different levels of consolidation through depth have on the dynamic response of the 3-D coupled system; and third, to study the effect of different geometries (depth) and properties (consolidation, compressibility and permeability) of the sediment layer on the system response.

In the following, the term "consolidated" will be used for the sediment when it can transmit shear waves. On the opposite, the term "non-consolidated" will be used when the shear-wave transmission capacity of the sediment is negligible. In order to asses the capabilities of the model and to analyse the different effects with a reasonable computational cost, a system whose geometry and boundary conditions are basically 2-D is studied first. Then, a fully 3-D arch dam-reservoir-foundation system where foundation radiation damping plays an important role is studied. Numerical results obtained for both geometries are analysed in order to show the influence of sediment material properties and geometry on the system response.

FORMULATION

Models used for the dynamic analysis of coupled systems that may consist of poroelastic, fluid and solid regions should be able to represent the dynamic behavior of

fluid-filled poroelastic regions, compressible fluid regions, viscoelastic solids, and the interaction between any two of these domains at interfaces.

The fluid (water in this study) is assumed to be inviscid and subject to small-motion pressure waves. Under these assumptions, the well known scalar integral equation formulation and a boundary element discretization can be established for this region to obtain a system of $\mathbf{N^w}$ equations which can be written [18] as:

$$\mathbf{H^w}\ \mathbf{p^w} = \mathbf{G^w}\ \mathbf{U_n^w} \tag{1}$$

where $\mathbf{N^w}$ is the number of nodes on the boundary; $\mathbf{U_n^w}$ is a vector containing the normal displacement of the water at boundary nodes; $\mathbf{p^w}$ is a vector containing nodal values of the pressure; and $\mathbf{H^w}$, $\mathbf{G^w}$ are $\mathbf{N^w} \times \mathbf{N^w}$ system matrices obtained by integration of the 3-D scalar time harmonic fundamental solution times the shape functions, over the boundary elements. The half space fundamental solution is used for free surface water regions; thus, the free surface boundary conditions are satisfied and no discretization of it is required.

Porous regions are assumed to be a fluid-filled poroelastic material governed by Biot's equations [14]. The constitutive equations are:

$$\tau_{ij} = \left(\lambda + \frac{Q^2}{R}\right) e\ \delta_{ij} + 2\ \mu\ \varepsilon_{ij} + Q\ \varepsilon\ \delta_{ij} \tag{2a}$$

$$\tau = Q\ e + R\ \varepsilon \tag{2b}$$

where: τ_{ij} are the solid skeleton stress components; τ is the fluid equivalent stress = $-\phi\ p$ (p = pore pressure); ϕ the porosity; ε_{ij} are solid skeleton strain components =

$1/2\left(u_{i,j}+u_{j,i}\right)$; δ_{ij} is the Kronecker delta function.; $e=\nabla\mathbf{u}$ and $\varepsilon=\nabla\mathbf{U}$ are the solid and fluid dilatation, respectively; $\mathbf{u}$ is the displacement of the solid; $\mathbf{U}$ is the displacement of the pore fluid; λ, μ are Lame constants for the drained solid skeleton; and Q, R are Biot constants.

The equilibrium equations in terms of the solid and fluid displacement for a time harmonic excitation of the type $e^{i\omega t}$ (ω = angular frequency), can be written as:

$$\mu\,\nabla^{2}\mathbf{u}+\nabla\left[\left(\lambda+\mu+\frac{Q^{2}}{R}\right)e+Q\,\varepsilon\right]+\mathbf{X}=-\omega^{2}\left(\hat{\rho}_{11}\,\mathbf{u}+\hat{\rho}_{12}\,\mathbf{U}\right) \qquad (3a)$$

$$\nabla\left[Q\,e+R\,\varepsilon\right]+\mathbf{X}'=-\omega^{2}\left(\hat{\rho}_{12}\,\mathbf{u}+\hat{\rho}_{22}\,\mathbf{U}\right) \qquad (3b)$$

where, in order to simplify the equations, the dissipation constant has been included as part of complex valued densities:

$$\hat{\rho}_{11}=\rho_{11}-i\,\frac{b}{\omega}\;\;;\;\;\hat{\rho}_{22}=\rho_{22}-i\,\frac{b}{\omega}\;\;;\;\;\hat{\rho}_{12}=\rho_{12}+i\,\frac{b}{\omega} \qquad (4)$$

$\mathbf{X}$ and $\mathbf{X}'$ are body forces in the solid and fluid phase, respectively; $\rho_{11}=(1-\phi)\,\rho_s+\rho_a$; $\rho_{22}=\phi\,\rho_f+\rho_a$; $\rho_{12}=-\rho_a$; ρ_s and ρ_f are solid and fluid phase densities, respectively ; ρ_a is the added density; $b=\dfrac{\gamma_f\,\phi^{2}}{k}$ is the dissipation constant; where k (m/s) is the hydraulic conductivity of the poroelastic medium and γ_f the specific weight of fluid phase.

The equilibrium equations can be written in terms of four variables, namely the solid displacement components and the fluid stress. Using equations (2b) and (3b), the fluid displacement can be written as

$$\mathbf{U} = -\frac{\nabla \tau + \mathbf{X}' + \omega^2 \hat{\rho}_{12} \mathbf{u}}{\omega^2 \hat{\rho}_{22}} \tag{5}$$

By substitution of (5) and (2b) into (3a) and taking the divergence of equation (3b) the following equilibrium equations in terms of only four variables are obtained:

$$\mu \nabla^2 \mathbf{u} + (\lambda + \mu) \nabla e + \left(\frac{Q}{R} - \frac{\hat{\rho}_{12}}{\hat{\rho}_{22}} \right) \nabla \tau + \left(\frac{\hat{\rho}_{11} \hat{\rho}_{22} - \hat{\rho}_{12}^2}{\hat{\rho}_{22}} \right) \omega^2 \mathbf{u} + \mathbf{X} - \frac{\hat{\rho}_{12}}{\hat{\rho}_{22}} \mathbf{X}' = \mathbf{0} \tag{6a}$$

$$\nabla^2 \tau + \omega^2 \frac{\hat{\rho}_{22}}{R} \tau + \omega^2 \left(\hat{\rho}_{12} - \frac{Q}{R} \hat{\rho}_{22} \right) e + \nabla \mathbf{X}' = 0 \tag{6b}$$

Internal damping of the solid skeleton can be introduced using a complex valued Lame constants μ of the type: $\mu = \text{Re}[\mu] (1+2i\xi)$; where ξ is the damping coefficient. A real valued Poissons' ratio yields a complex valued Lame constant λ of the same type as μ.

By substitution of plane wave expressions for $\mathbf{u}$ and τ into Equation (6) for zero body forces, a characteristic equation for the wave numbers is obtained. Three solutions of that equation exist corresponding to three kinds of time harmonic plane waves. One is a shear wave transmitted through the solid skeleton. The other two are dilatational waves (P1 and P2). All wave velocities are complex and frequency dependent; i.e. they are dissipative and dispersive. The solid and the fluid dilatation are in phase for the long longitudinal waves (P1) and they are in opposite phase for the short waves (P2), which damps out at short distance from the perturbation.

The reciprocity relation between two dynamic poroelastic states defined in a domain Ω with boundary Γ, in terms of four independent solid and fluid variables, were first obtained by Domínguez [15,16] and Cheng et al. [17]. Both formulations are equivalent

although some differences exist between them: on the one hand the chosen variables are different; on the other hand, the integral equation is obtained from a reciprocal theorem in [17] whereas a weighted residual formulation from equilibrium equations is used in [15,16]. The weighted residual formulation, however, can be written in a more general form from governing equations. Thus, starting from (6), in condensed form and index notation:

$$G_i + F_i = 0 \atop H + X'_{i,i} = 0 \quad ; \quad {G_i = \mu\, u_{i,jj} + (\lambda + \mu)\, u_{j,ij} + \left(\dfrac{Q}{R} - \dfrac{\hat{\rho}_{12}}{\hat{\rho}_{22}}\right)\tau_{,i} + \left(\dfrac{\hat{\rho}_{11}\,\hat{\rho}_{22} - \hat{\rho}_{12}^2}{\hat{\rho}_{22}}\right)\omega^2 u_i \atop H = \tau_{,ii} + \omega^2\,\dfrac{\hat{\rho}_{22}}{R}\,\tau + \omega^2\left(\hat{\rho}_{12} - \dfrac{Q}{R}\,\hat{\rho}_{22}\right)u_{i,i}} \tag{7}$$

and $F_i = X_i - Z\,X'_i,\ \left(Z = \dfrac{\hat{\rho}_{12}}{\hat{\rho}_{22}}\right)$; weighting the first equation with displacement functions u^*_i and the second with τ^*, adding the two equations and integrating over domain Ω:

$$\int_\Omega \left[\left(G_i + F_i\right)u^*_i + \left(H + X'_{i,i}\right)\tau^*\right] d\Omega = 0 \tag{8}$$

by using integration by parts and the divergence theorem, the following reciprocal relation can be obtained:

$$\int_\Gamma t_i\, u^*_i\, d\Gamma + \int_\Gamma \tau\left(U^*_n + J\,X'^*_i\, n_i\right)d\Gamma + \int_\Omega \left(F_i\, u^*_i + J\,X'_{i,i}\,\tau^*\right)d\Omega =$$
$$= \int_\Gamma t^*_i\, u_i\, d\Gamma + \int_\Gamma \tau^*\left(U_n + J\,X'_i\, n_i\right)d\Gamma + \int_\Omega \left(F^*_i\, u_i + J\,X'^*_{i,i}\,\tau\right)d\Omega \tag{9}$$

where, $t_i = \tau_{ij} n_j$ are the traction components on the solid phase, $U_n = U_i n_i$ is the normal

displacement of the fluid, and $J = \dfrac{1}{\omega^2 \hat{\rho}_{22}}$. Obviously, the above equation is equivalent

to the equations proposed in [15,16], although Equation (9) is a more compact and easy

form. The use of a weighted residual procedure allows to obtain expressions of the

integral equation where the weighting fields do not necessary have to verify the

governing equation of the real fields, neither its constitutive equations (e.g. [19]). This

fact, however, doesn't represent any real advantage in the present formulation.

By using two fundamental solutions, one corresponding to a unit point load in the solid

phase, and the other to a unit point source in the fluid, for 3-D problems under zero

body forces conditions ($X_i = 0$; $X'_i = 0$), the following boundary integral equations are

obtained [15,16]

$$\mathbf{c}^k \mathbf{u}^k + \int_\Gamma \mathbf{p}^* \mathbf{u} \, d\Gamma = \int_\Gamma \mathbf{u}^* \mathbf{p} \, d\Gamma \tag{10}$$

where, $\mathbf{u}$ and $\mathbf{p}$ are boundary variables vectors:

$$\mathbf{u} = \begin{Bmatrix} u_1 \\ u_2 \\ u_3 \\ \tau \end{Bmatrix} \qquad \mathbf{p} = \begin{Bmatrix} t_1 \\ t_2 \\ t_3 \\ U_n \end{Bmatrix} \tag{11}$$

$\mathbf{u}^*$ and $\mathbf{p}^*$ are fundamental solution tensors:

$$\mathbf{u}^* = \begin{bmatrix} u_{11}^* & u_{12}^* & u_{13}^* & -\tau_1^* \\ u_{21}^* & u_{22}^* & u_{23}^* & -\tau_2^* \\ u_{31}^* & u_{32}^* & u_{33}^* & -\tau_3^* \\ u_{o1}^* & u_{o2}^* & u_{o3}^* & -\tau_o^* \end{bmatrix} \qquad \mathbf{p}^* = \begin{bmatrix} t_{11}^* & t_{12}^* & t_{13}^* & -U_{n1}^* \\ t_{21}^* & t_{22}^* & t_{23}^* & -U_{n2}^* \\ t_{31}^* & t_{32}^* & t_{33}^* & -U_{n3}^* \\ t_{o1}^* & t_{o2}^* & t_{o3}^* & -\hat{U}_{no}^* \end{bmatrix} \tag{12}$$

and $\mathbf{c}^k$ is the local free term at collocation point $\mathbf{x}_k$ with the form:

$$\mathbf{c}^k = \begin{bmatrix} c_{11}^e & c_{12}^e & c_{13}^e & 0 \\ c_{21}^e & c_{22}^e & c_{23}^e & 0 \\ c_{31}^e & c_{32}^e & c_{33}^e & 0 \\ 0 & 0 & 0 & Jc^p \end{bmatrix}^k \qquad (13)$$

where c_{ij}^e are the same as the free terms for the elastic static equations at collocation

point $\mathbf{x}_k$, and c^p is the same as the scalar static term at $\mathbf{x}_k$.

The fundamental solution terms are obtained using the thermo-elastic analogy and

Kupradze's et al. [20] solution for that kind of problems. They are given in [11].

A boundary element discretization of Equation (10) leads to a system of $4\,\mathbf{N^p}$ equations:

$$\mathbf{H^p u^p = G^p\ p^p} \qquad (14)$$

where $\mathbf{N^p}$ is the number of nodes on the boundary; $\mathbf{u^p}$ is a vector containing solid

displacement and fluid stress at boundary nodes; $\mathbf{p^p}$ is a vector containing solid traction

and fluid normal displacement at boundary nodes; and $\mathbf{H^p}$, $\mathbf{G^p}$ are $\mathbf{4N^p \times 4N^p}$ system

matrices obtained by integration of the 3-D time harmonic poroelastic fundamental

solution times the shape functions, over the boundary elements.

The time-harmonic behavior of the solid viscoelastic regions of the problem are also

represented using boundary elements based on the integral equation formulation for this

kind of material. A system of $3\,\mathbf{N^s}$ equations is obtained.

$$\mathbf{H^s u^s = G^s\ p^s} \qquad (15)$$

where $\mathbf{N}^s$ is the number of nodes on the boundary; $\mathbf{u}^s$ is a vector containing displacement at boundary nodes; $\mathbf{p}^s$ is a vector containing traction at boundary nodes; and $\mathbf{H}^s, \mathbf{G}^s$ are $\mathbf{3N^s \times 3N^s}$ system matrices obtained by integration of the 3-D time harmonic elastic fundamental solution times the shape functions, over the boundary elements.

There are six kinds of interfaces in the problem at hand: poroelastic-viscoelastic, water-poroelastic, water-viscoelastic, poroelastic-poroelastic, water-water and viscoelastic-viscoelastic. The compatibility and equilibrium conditions along the interfaces are detailed in Table 1, where $\mathbf{n}$ is the normal unit vector to the interface and super-indexes *s*, *w* and *p* denote viscoelastic solid, water region and poroelastic material, respectively. These interface conditions for six different situations are enough to define a well-posed problem in each case.

Most dynamic soil-structure interaction problems include semi-infinite regions where the radiation damping plays an important role. The boundary element technique is able to represent these regions and the radiation damping very simply. The boundaries of the semi-infinite regions are left open at a certain distance from the zone of interest. The radiation damping is automatically represented since fundamental solutions satisfy radiation conditions [18].

SIMPLE DYNAMIC SEDIMENTS-FLUID-STRUCTURE INTERACTION PROBLEM

A coupled problem with a simple geometry including water, viscoelastic solid and fluid filled poroelastic solid is analyzed in this section. This numerical experiment is intended

to understand the dynamic behavior of the coupled system, to explain the wave propagation mechanisms appearing in it, and to asses some of the parameters related to sediment effects on the seismic response of 3-D arch dams. A parametric study including the influences of degree of saturation, permeability, heterogeneity and degree of consolidation of the bottom sediment is carried out.

Problem definition

A very simple 3-D water reservoir with the cross section shown in Figure 1 is studied. The reservoir is 100 m long, 100 m deep and 20 m wide. It is closed on one side by a 100 x 20 x 20 m concrete wall with properties: density $\rho_d = 2481.5$ Kg/m^3, Poisson's Ratio $\upsilon_d = 0.2$, Shear Modulus $\mu_d = 11500$ MPa and internal damping $\xi_d = 0.05$. The water is considered as an inviscid fluid with wave propagation velocity $c_w = 1438$ m/s and density $\rho_w = 1000$ Kg/m^3. Part of the reservoir up to a height h, is full with bottom sediment whose behavior depends on its degree of consolidation.

Consolidated sediment model

The consolidated sediment is represented as a water saturated poroelastic domain (Biot [14]). A uniform sediment is first assumed (variable properties through depth will be considered later). The sediment properties, as taken from [8], are: porosity $\phi = 0.6$, shear modulus of the solid skeleton $\mu_s = 7.7037 \times 10^6$ N/m^2, Poisson's Ratio $\upsilon_s = 0.35$, internal damping $\xi_s = 0.05$, solid particles density $\rho_s = 2640$ Kg/m^3, water density $\rho_w = 1000$ Kg/m^3, added density $\rho_a = 0$, and dissipation constant $b = 3.5316 \times 10^6$ Ns/m^4 (corresponding to a hydraulic conductivity $k = 10^{-3}$ m/s).

Biot's constants Q and R are obtained with the hypothesis of very high stiffness of the solid particles; thus, $Q = (1- \phi) K_f$ and $R = \phi K_f$, K_f being the fluid compressibility ($K_f = 2.0736 \times 10^9$ N/m^2 when there are not gas particles in the water).

Boundary element discretizations of one half of the problem are shown in Figures 2a and 2b for sediment depths h/H = 0.2 and 0.4, respectively. Symmetry conditions are taken into account by the numerical code. The bottom and right hand side boundaries, where horizontal or vertical time harmonic motions are prescribed, are rigid and impervious. Boundary conditions for a horizontal excitation are also shown in Figure 2. Nine-node quadratic elements are used for all boundaries. No discretization is needed on the water free surface since the half-space fundamental solution is used for this region. The size of the elements in each region is determined by the corresponding wavelength. In the present model the elements at the boundary of the porous sediments are 10×10 m, whereas elements in the wall (viscoelastic region) or water are four times larger (20×20 m). The use of discontinuous elements simplifies the mesh definition and the application of integral equations in each boundary. Since one of the purposes of the present paper is testing 3-D boundary element models for coupled systems, the models shown in Fig.2 are three-dimensional, in spite of the fact that the simple geometry and boundary conditions on the side walls (see Fig.2) would allow for the use of a 2-D boundary element representation. All results presented in the following have been obtained with the 3-D representation and have been validated by comparison with those obtained using a 2-D boundary element model [10]. Both sets of results fully coincide in all cases. The representative variable for the dynamic behavior of the model is the amplification at the central point of the wall upper face (node "i" in Fig.2), when a unit

time harmonic displacement in horizontal or vertical direction is prescribed to the rigid boundaries. The frequency (ω) is normalized by the first natural frequency of the concrete wall on rigid foundation (ω_1).

Consolidated sediment model - Influence of porous material saturation degree

The existence of gas particles in the pore water of the porous solid changes its effective bulk modulus according to the following equation presented by Verruijt [21]

$$\frac{1}{K'_f} = \frac{1}{K_f} + \frac{1-s}{p^o}$$

(16)

where K'_f is the bulk modulus under partially saturated conditions, s the degree of saturation and p^o the hydrostatic pressure. The variation of the pore-fluid compressibility produces changes of different significance on the three wave propagation velocities of the porous medium. Figure 3 shows these changes for the three types of waves, saturation degree from 100% to 99%, p^o corresponding to 80 and 90 m depth (sediment thickness h = 40 and 20 m, respectively) and an intermediate angular frequency value in the studied frequency range (four times the first natural frequency of the concrete wall). It can be seen from the figure that the saturation degree clearly modifies the modulus of the P1 wave velocity but not that of the other two waves (P2 and S). It is worth to check how the change on the P1 wave velocity associated to saturation degree modifies the system response to a harmonic horizontal motion. Figure 4 shows the modulus of amplification at the wall top versus the dimensionless frequency ω/ω_1 for a horizontal excitation, full reservoir conditions, three degrees of saturation (100%, 99.95% and 99.5%), and two values of the sediment

thickness (h/H = 0.2 and 0.4). The first natural frequency and the first peak amplitude change very little in all cases. However, the response is clearly influenced by the saturation degree of the sediment for higher values of ω/ω_1. The fully saturated sediment only produces a certain shift of the second and third peaks whereas the partially saturated sediment (even the cuasi-saturated one s = 0.9995) completely modifies the response after the first peak. A similar behavior is observed for vertical excitation of the base (not shown). It should be concluded that sediment compressibility must be carefully evaluated.

In order to see how changes in sediment saturation alter the hydrodynamic pressure in the system the pressure at a point on the wall face at a depth z = 0.6 H, has been represented versus frequency in Figure 5 for vertical excitation, sediment thickness h = 0.2 H and three situations: no sediment, fully saturated sediment and 99.5% partially-saturated sediment. It is clearly seen in the figure that the effect of the fully saturated sediment is only a small shift of the resonance peaks. The pressure for partially saturated sediment is significantly different to that of the no sediment situation for all the frequency range. The first peak of the coupled system (shown in Figure 4) was not changed significantly by the partially saturated sediment because it is mainly associated to the wall first natural frequency.

Consolidated sediment model - Influence of sediment permeability

To study the influence of sediment permeability on the dynamic response, a brief analysis of its effects on the characteristics of the waves in the sediment is done first. Variation of the P1 and S wave propagation velocity of the order of 20% exist for the permeability range shown in Figure 6, where wave velocity amplitude variation for two

saturation degrees is shown. The short wave velocity (P2) presents the most important changes with permeability. It can be seen from the figure that this velocity grows very fast for hydraulic conductivity between 5×10^{-3} m/s and 5×10^{-1} m/s; P2-wave velocity being bigger than S–wave velocity for values greater than 5×10^{-2} m/s. The wave velocity variations shown in Fig.6 have been obtained for a frequency equal to four times the fundamental frequency of the concrete wall. Results for other frequencies are similar. Little influence of the sediment permeability can be expected for values of k below 10^{-3}. To test the two extreme situations indicated by Fig.6, a sediment thickness h = 0.4 H, two hydraulic conductivities values $k = 10^{-3}$ m/s and $k = 1$ m/s, and two saturation degrees, were considered for the problem at hand. Amplification at the top of the wall for horizontal excitation is shown in Figure 7. It is seen that permeability effect is very small for the fully saturated sediment (Figure 7a). It does not change the first resonance peak and only changes slightly the upper peaks. In the partially saturated case (99.5%) shown in Figure 7b, no change is noticed in the first resonance peak and the main influence of a permeability increase is a reduction of the sediment damping effect for frequencies higher than the first resonance peak, in particular for the second and third peaks. Notice that the change in the P2 wave velocity has an important influence on the local response of the sediment even in the fully saturated case but not on the wall response. Figure 8a shows the vertical displacement amplitude of the solid skeleton of the fully saturated sediment at a point on the water-sediment interface at a distance d = 60 m from the wall face when a unit vertical displacement is prescribed at the bottom. These displacement values depend very much on permeability and are very close, except for the small secondary peaks, to those predicted by the exact solution of the 1-D problem of a uniform water layer on a fully saturated sediment layer. Nevertheless,

hydrodynamic pressure at water-sediment interface present very little variation with permeability (Fig.8b) and so does the hydrodynamic pressure at d = 0 at water-sediment interface (results not shown), and the vertical displacement of the skeleton at the sediment-wall interface d = 0 (Fig.8c). This facts lead to a little dependence of the wall response on the fully saturated sediment permeability in spite of the important changes observed on the motion of the skeleton away from the wall. In the partially saturated sediment case (Fig.8d) changes in permeability produce changes in the amplitude of resonance peaks of the hydrodynamic pressure that eventually lead to the variations in the wall response already shown in Fig.7b.

Consolidated sediment model - Influence of sediment heterogeneity

Sediments are consequence of a settling process where gravity plays a key role. There is certain level of uncertainty about the actual mechanical properties of the resulting medium and consequently about the type of mechanical model most appropriate to represent its behaviour. It is worth to study the influence of the gradient of the sediment mechanical properties and its level of consolidation on the system dynamic response. The effect of the first of these two factors is studied in the present section and the second in the next one. Assume a graded consolidated porous sediment layer of depth h = 0.4 H whose mechanical properties vary with depth from those of water, at the water sediment interface, to those assumed for the porous sediment of the previous analysis at the bottom level. Due to the lack of a fundamental solution for graded saturated porous materials, the sediment will be represented by four uniform layers with different properties. All of them are modelled as Biot's porous saturated domains. Figure 9 shows the boundary element discretization used for this case. The depth varying mechanical

properties are given for the four layers in Figure 10. Other properties; i.e., ν, ρ_s, ρ_f and ρ_a, are kept constant through depth and their values are equal to those assumed in the previous analysis. The effect of the sediment heterogeneity on the response is shown in Figures 11a, 11b and 11c for sediments with a 100%, 99.95% and 99.5% saturation degree at the bottom level, respectively. Note that the saturation degree in the last two cases (Figures 11b and 11c) vary from 100% at the water-sediment interface to 99.95% and 99.5%, respectively, at the bottom level. It can be concluded from the figures that the gradient of the sediment properties does not produce relevant effects for fully saturated sediments; only a small shift in the second and third resonant frequencies (Figure 11a). Changes with depth of the sediment properties have significant effects on the system response for non-saturated sediments. These effects are more important as the saturation degree decreases (Figures 11b and c). No differences are observed next to the first resonant frequency in all cases.

Influence of sediment consolidation degree

The system response for three different sediment strata will be studied in this section. The first case corresponds to the stratum with four poroelastic layers, whose properties are given in Figure 10, and has been studied in the previous section. For the second case ("partially consolidated sediment") it is assumed that the two upper layers behave as scalar media as they are not consolidated. The material of these layers is not able to transmit shear waves. The two lower layers have certain elastic properties and behave as Biot's poroelastic media. Mechanical properties for the four different layers are given in Figure 12a. The third stratum considered ("non-consolidated sediment"), consist of four uniform layers whose density increases with depth. In this case it is assumed that none

of the layers can transmit shear waves and that the only effect of sedimentation is increasing the material density. Mechanical properties for this case are given in Figure 12b. The boundary element discretization for the three cases is the same used before (Figure 9). Figure 13a shows the amplification of the base motion at the top of the wall for the three 100% saturated sediment models (consolidated, partially consolidated and non-consolidated) when a time harmonic horizontal motion is prescribed at the bottom of the model. These results show that the type of sediment has little influence on the response at the top of the wall. Only the model corresponding to sediments without any shear wave transmission capacity yield a slightly different response with higher amplification at the upper resonant peaks.

The existence of a little amount of gas in the sediment can only be explained when a solid skeleton exist; i.e. when a two-phase poroelastic material is assumed (consolidated or partially consolidated), and not when the sediment behaves as a liquid with increasing density (non-consolidated). Therefore, partial saturation is only assumed when the sediment has certain level of consolidation and a Biot poroelastic model is used to represent its behaviour. The effects of the consolidation level for two partially saturated sediments are shown in Figures 13b and 13c. In the consolidated case the four layers of sediment are poroelastic solids whereas in the partially consolidated case only the two lower layers are assumed to behave as poroelastic solids. In both cases, the saturation degree decreases from 100% at top of the sediment to 99.95% or 99.5% at bottom level (Figures 13b and 13c, respectively). It can be observed from Figures 13b and 13c that there is a significant influence of the consolidation degree on the dynamic response when there is a certain amount of gas trapped in the sediment. This influence

is more important as the excitation frequency increases and the saturation degree decreases.

3-D SEDIMENT-FLUID-STRUCTURE INTERACTION PROBLEM. DYNAMIC RESPONSE OF ARCH DAMS.

It is important to analyse some of the factors studied in the previous sections for a more realistic coupled system that behaves in a really 3-D manner. To do so, a purely 3-D dynamic interaction problem is study in this section using the same Boundary Element code as above. The seismic response of an arch dam-reservoir-sediment-foundation rock system (Fig. 14) is evaluated to S and P time-harmonic plane waves impinging vertically the model from infinity. Other important phenomena such radiation damping and space distribution of excitation take place in this 3-D problem, in opposition to the previous 2-D simplified coupled problem. The 142 m high Morrow Point Dam, witch geometry is taken from [22,23] has been chosen for the present analysis. The BE discretization used is shown in Fig.14 (all the regions of the system are discretized into boundary elements) where it can be observed that geometrical symmetry has been taken into account. Dam and foundation rock are viscoelastic solids, water is a compressible fluid and sediment is a Biot's homogeneous poroelastic layer with a thickness equal to 20% of the maximum dam height and extending in the upstream direction up to 172 m from the dam. The properties of the concrete dam, water and porous sediments are the same as the concrete wall, water and porous sediment in the simplified coupled problem previously analyzed, respectively. The foundation rock is also assumed to be a linear viscoelastic solid with the same shear modulus, Poisson's ratio and damping ration as the dam and density 2641.65 kg/m^3. The geometry shown in Figure 14 corresponds to a

case of a very long water reservoir. The reservoir boundary of a zone close to the dam, that can be rather extensive and irregular, is discretized into elements. The rest of the reservoir is assumed to be a uniform section infinite channel. A closing boundary taking into account the hydrodynamic wave radiation is located at that point [12]. Figures 15a and 15b show the amplitude of the upstream acceleration of a point located at the dam crest on the plane of symmetry, for an upstream excitation (S-wave) and vertical excitation (P-wave), respectively, versus the dimensionless frequency ω/ω_1, where ω_1 is the fundamental resonant frequency of the dam-on-rigid-foundation and empty-reservoir conditions for a symmetric mode. Three different situations are represented: full reservoir with no sediment; full reservoir with a fully saturated bottom sediment layer; and full reservoir with a partially saturated (99.5%) bottom sediment layer. It can be seen from the figure that the existence of fully saturated sediment has very little influence on the dam response. However, the existence of a partially saturated sediment layer changes significantly the hydrodynamic pressure in the reservoir and consequently the dam response: reduces the first natural frequency and the peak amplitude at that frequency, changes the position of other natural frequencies and reduces the system amplification except for the second and third peaks of the upstream excitation case. One can conclude that the seismic analysis of 3-D arch dams-reservoir systems requires the identification of bottoms sediments and the adequate evaluation of their properties (in particular the compressibility) and the use of a numerical model with include the proper representation of each region of the system (dam, water, sediments and foundation rock) the interaction effects between any two of them and the spatial character of seismic excitation. A more extensive study of this kind of 3-D coupled systems can be found in [11].

CONCLUSIONS

A three-dimensional boundary element technique for dynamic analysis of coupled systems that may consist of water or any other pressure-wave propagating material, viscoelastic solids and fluid-filled poroelastic regions has been presented in this paper. The boundary element formulation for wave propagation in poroelastic solids has been reviewed to include a weighted residual formulation more general and concise than those existing in the literature.

The present model is particularly well suited for the analysis of dam-foundation reservoir systems. It includes homogeneous or layered sediments which are represented as a two-phase fluid-filled poroelastic medium, as a scalar domain with no shear waves, or as a combination of both. It allows for the evaluation of the effects of bottom sediments with different properties on the dynamic response of dams and other containment structures. Interaction effects are taken into account in a rigorous way. A problem with simple geometry has been studied to asses the importance of absorption of hydrodynamic pressure waves by the underlying bottom sediments and the capability of the BE model to represent it properly. Sediments of three different kinds have been assumed: consolidated sediments represented as a Biot fluid-filled porous material; non-consolidated sediments represented as a pressure-wave only propagating material; and semi-consolidated sediments represented by one or several layers of non-consolidated sediments and one or several layers of consolidated sediments with different saturation degree and permeability.

The obtained results show a good representation of the interaction phenomena and the dynamic response of this type of 3-D problems. The following conclusions regarding

the effects of bottom sediment material and its boundary element representation, can be drawn from the results obtained with both the simple and the fully 3-D model.

In the case of consolidated sediments, compressibility plays a key role on the dynamic response of couple systems of this type. Existence of gas particles in bottom sediments highly influences this parameter, and consequently the system response. Fully saturated sediments have little influence on the system response, in particular for low and intermediate frequencies, whereas partially saturated sediments produce important changes in the response. These changes significantly depend on the sediment thickness and properties, being different for layered than for homogeneous sediments. Permeability of partially saturated sediments has an important effect on the system response. Changes in permeability do not change to a significant extent the resonance frequencies of the system but modify the damping effect of the sediment by changing the peaks amplitude. An increase of permeability leads to an increase of the higher mode peaks amplitude.

The consolidation degree does not play an important role as long as the sediment is fully saturated. Partially saturated sediments may induce a different response of the system depending on their consolidation degree.

ACKNOWLEDGEMENTS

REFERENCES

1. Medina F, Domínguez J, Tassoulas JL. Response of dams to earthquake including effects of sediments. *Journal of Structural Engineering* (ASCE) 1990; **116**(1):3108-3121.

2. Zhao C. Effects of reservoir bottom sediments on hydrodynamic pressure of gravity dams. *Computer & Structures* 1994; **52**(2):297-307.

3. Zhao C, Xu TP, Valliapan S. Seismic response of concrete gravity dams including water-dam-sediment-foundation interaction. *Computer & Structures* 1995; **54**(4):705-715.

4. Chuhan Z, Chengda Y, Guanglun W. Numerical simulation of reservoir sediment and effects on hydro-dynamic response of arch dams. *Earthquake Engineering and Structural Dynamics* 2001; **30**:1817-1837.

5. Cheng AHD. Effects of sediments on earthquake induced reservoir hydrodynamic response. *Journal of Engineering Mechanics* (ASCE) 1986; **112**(7):645-665.

6. Bougacha S, Tassoulas JL. Effects of sedimentary material on the response of concrete gravity dams. *Earthquake Engineering and Structural Dynamics* 1991;**20**:849-858.

7. Bougacha S, Tassoulas JL. Seismic response of gravity dams I: Modeling of sediments. *Journal of Engineering Mechanics* (ASCE) 1991; **117**(8):1826-1837.

8. Bougacha S, Tassoulas JL. Seismic response of gravity dams II: Effects of sediments. *Journal of Engineering Mechanics* (ASCE) 1991; **117**(8):1839-1850.

9. Chen BF, Hung TK. Dynamic pressure of water and sediment on rigid dam. *Journal of Engineering Mechanics* (ASCE) 1993; **119**(7):1411-1434.

10. Domínguez J, Gallego R, Japón BR. Effects of porous sediments on seismic response of concrete gravity dams. *Journal of Engineering Mechanics* (ASCE) 1997; **123**(4):302-311.

11. Maeso O, Aznárez JJ, Domínguez J. Three-dimensional models of reservoir sediment and effects on the seismic response of arch dams. *Earthquake Engineering and Structural Dynamics* 2004; **33**:1103-1123.

12. Domínguez J, Maeso O. Earthquake analysis of arch dams II: dam-water-foundation interaction. *Journal of Engineering Mechanics* (ASCE) 1993; **119**(3):513-530.

13. Maeso O, Aznárez JJ, Domínguez J. Effects of the space distribution of the excitation on the seismic response of arch dams. *Journal of Engineering Mechanics* (ASCE) 2002; **128**(7):759-768.

14. Biot MA. The theory of propagation of elastic waves in a fluid-saturated porous solid I. Low frequency range. *Journal of Acoustical Society of America* 1956; **28**: 168-178.

15. Domínguez J. An integral formulation for dynamic poroelasticity. *Journal of Applied Mechanics* (*ASME*) 1991; **58**: 588-591.

16. Domínguez J. Boundary element approach for dynamic poroelastic problems. *International Journal for Numerical Methods in Engineering* 1992; **35**: 307-324.

17. Cheng AHD, Badmus T, Beskos DE. Integral equation for dynamic poroelasticity in frequency domain with BEM solution. *Journal of Engineering Mechanics* (*ASCE*) 1991; **117**(5): 1136-1157.

18. Domínguez J. *Boundary elements in dynamics*. Computational Mechanics Publications: Southampton & Elsevier Applied Science: New York, 1993.

19. Chen J, Dargush GF. Boundary element method for dynamic poroelastic and thermoelastic analyses. *International Journal of Solids & Structures* 1995; **32**(15): 2257-2278.

20. Kupradze VD, Gegelia TG, Basheleishvili MO, Burchuladze TV. *Three-dimensional problems of the mathematical theory of elasticity and thermoelasticity.* North-Holland: Amsterdam, 1979.

21. Verruijt A. Elastic storage of aquifers. *Flow through porous media.* R.J.M. de Weist, ed., Academic Press Inc., San Diego, Calif.

22. Hall JF, Chopra AK. Dynamic analysis of arch dams including hydrodynamic effects. *Journal of Engineering Mechanics* (ASCE) 1983; **109**: 149-163.

23. Fok KL, Chopra AK. Frequency response functions of arch dams: hydrodynamic and foundation flexibility effects. *Earthquake Engineering and Structural Dynamics* 1986; **14**: 769-795.

Kind of interface	Equilibrium equations	Compatibility equations
viscoelastic solid (^{s1}) - viscoelastic solid (^{s2})	$\mathbf{t}^{s1} + \mathbf{t}^{s2} = \mathbf{0}$	$\mathbf{u}^{s1} = \mathbf{u}^{s2}$
water (^{w1}) - water (^{w2})	$p^{w1} = p^{w2}$	$U_n^{w1} + U_n^{w2} = 0$
viscoelastic solid (^{s}) -water (^{w})	$\mathbf{t}^s - p^w \mathbf{n}^w = \mathbf{0}$	$\mathbf{u}^s \mathbf{n}^s + U_n^w = 0$
poroelastic material (^{p}) - viscoelastic solid (^{s})	$\mathbf{t}^s + \mathbf{t}^p + \tau^p \mathbf{n}^p = \mathbf{0}$	$\mathbf{u}^s = \mathbf{u}^p$ $\mathbf{u}^p \mathbf{n}^p = U_n^p$
poroelastic material (^{p}) – water (^{w})	$-\dfrac{\tau^p}{\phi} = p^w$ $\mathbf{t}^p - (1-\phi) p^w \mathbf{n}^w = \mathbf{0}$	$U_n^w + \left[\mathbf{u}^p \mathbf{n}^p (1-\phi) + U_n^p \phi\right] = 0$
poroelastic material (^{p1})– poroelastic material (^{p2})	$\dfrac{\tau^{p1}}{\phi^{p1}} = \dfrac{\tau^{p2}}{\phi^{p2}}$ $\mathbf{t}^{p1} + \tau^{p1} \mathbf{n}^{p1} + \mathbf{t}^{p1} + \tau^{p2} \mathbf{n}^{p2} = \mathbf{0}$	$\mathbf{u}^{p1} = \mathbf{u}^{p2}$ $\phi^{p1}\left[U_n^{p1} - \mathbf{u}^{p1}\mathbf{n}^{p1}\right] +$ $\phi^{p2}\left[U_n^{p2} - \mathbf{u}^{p2}\mathbf{n}^{p2}\right] = 0$

Table 1. Interface equilibrium and compatibility conditions.

	μ (N/m^2)	ϕ	s	k (m/s)	b (N s /m^4)	Q (N/m^2)	R (N/m^2)
S1	1.1005×10^6	0.943	1.0	1.0	8.7235×10^3	1.1820×10^8	1.9554×10^9
			0.99993			9.6279×10^7	1.5928×10^9
			0.9993			3.6075×10^7	5.9682×10^8
S2	3.3016×10^6	0.829	1.0	10^{-1}	6.7418×10^4	3.5459×10^8	1.7190×10^9
			0.99979			2.2274×10^8	1.0799×10^9
			0.9979			5.1252×10^7	2.4847×10^8
S3	5.5026×10^6	0.714	1.0	10^{-2}	5.0011×10^5	5.9305×10^8	1.4806×10^9
			0.99964			3.1291×10^8	7.8119×10^8
			0.9964			5.9588×10^7	1.4876×10^8
S4	7.7037×10^6	0.6	1.0	10^{-3}	3.5316×10^6	8.2944×10^8	1.2442×10^9
			0.9995			3.9263×10^8	5.8895×10^8
			0.9950			6.8408×10^7	1.0261×10^8

Table 2. Mechanical properties for porous sediment layers and three different saturation degrees.

	S3	S4
μ (N/m^2)	2.5679×10^6	7.7037×10^6
ϕ	0.714	0.6
s	1.0	1.0
	0.9998	0.9995
	0.9983	0.9950
k (m/s)	10^{-1}	10^{-3}
b (N s/m^4)	5.0011×10^4	3.5316×10^6
Q (N/m^2)	5.9305×10^8	8.2944×10^8
	4.1685×10^8	3.9263×10^8
	1.1345×10^8	6.8408×10^7
R (N/m^2)	1.4806×10^9	1.2442×10^9
	1.0407×10^9	5.8895×10^8
	2.8322×10^8	1.0261×10^8

Table 3. Mechanical properties for poroelastic material layers in partially consolidated stratum (Figure 12a).
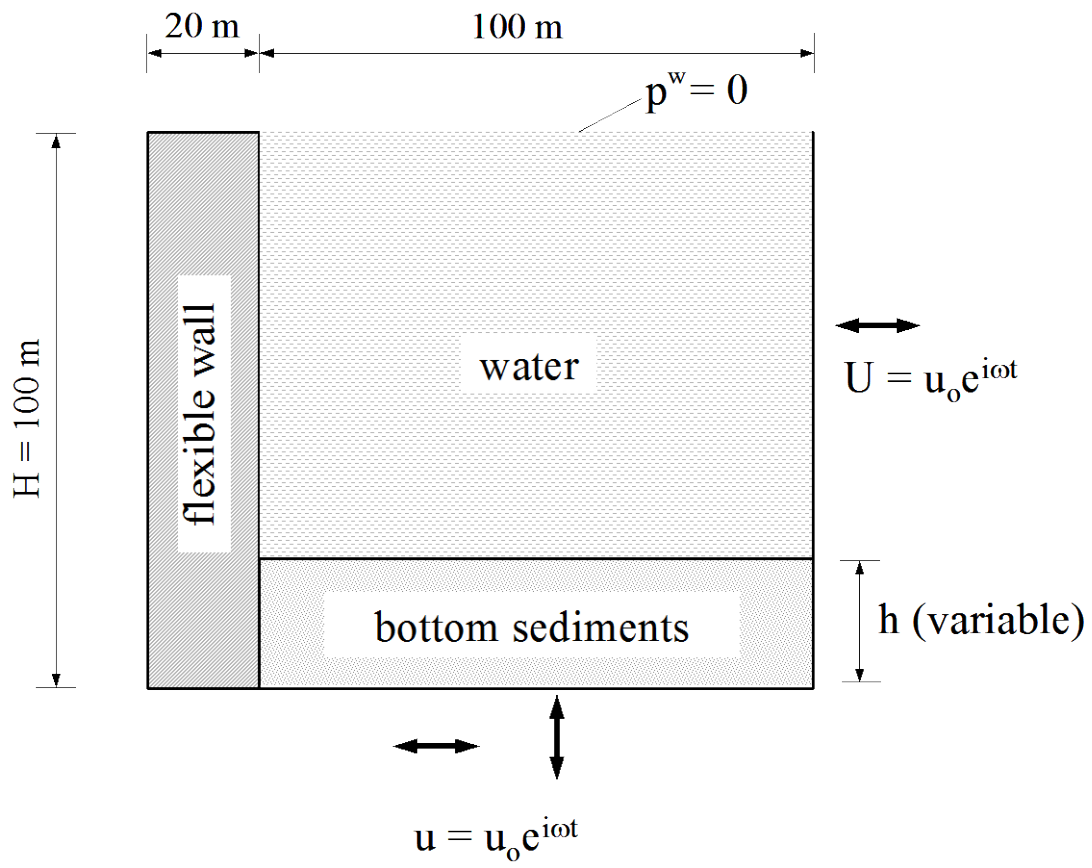
Figure 1. Simple coupled problem description.

Figure 2. Simple coupled problem. Boundary Element discretizations and boundary conditions.
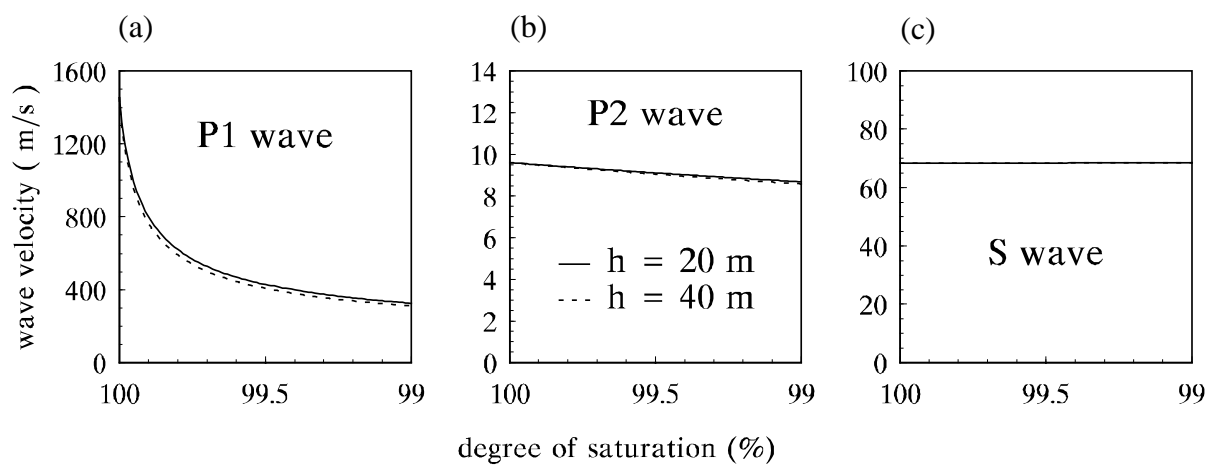
Figure 3. Wave propagation velocity amplitudes in the sediment vs. degree of saturation.
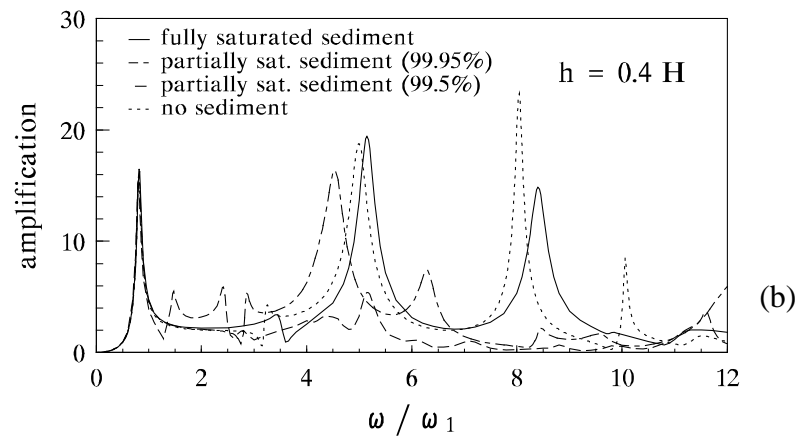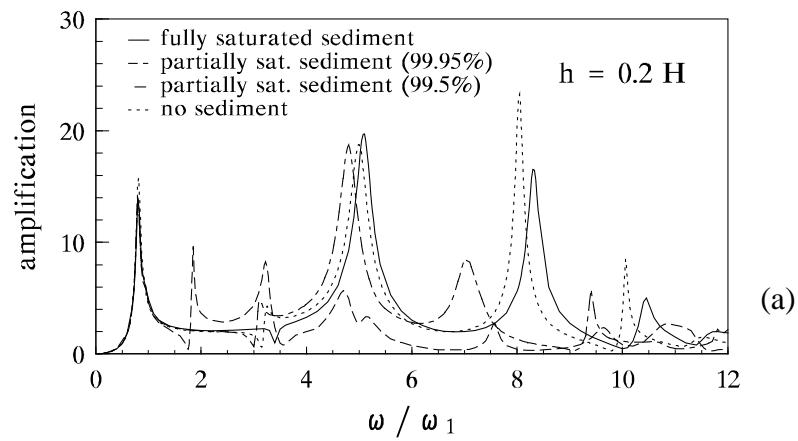
Figure 4a, b. Influence of sediment saturation degree. Horizontal amplification at the wall top to horizontal excitation for sediment thickness h/H = 0.2 and 0.4.
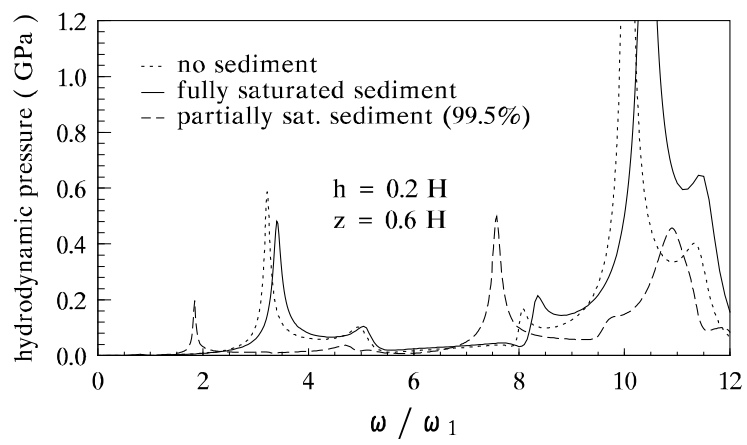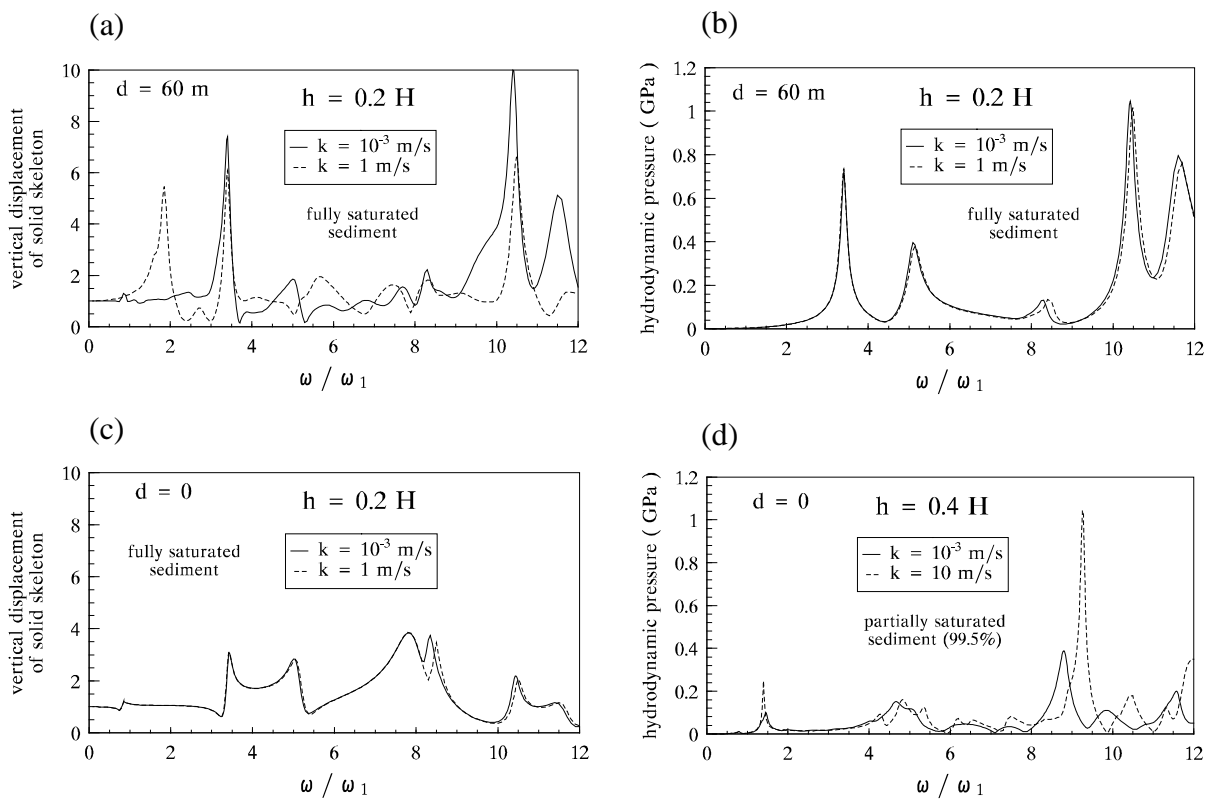
Figure 5. Influence of sediment saturation degree.
Hydrodynamic pressure at z = 0.6H on the wall face. Vertical excitation.
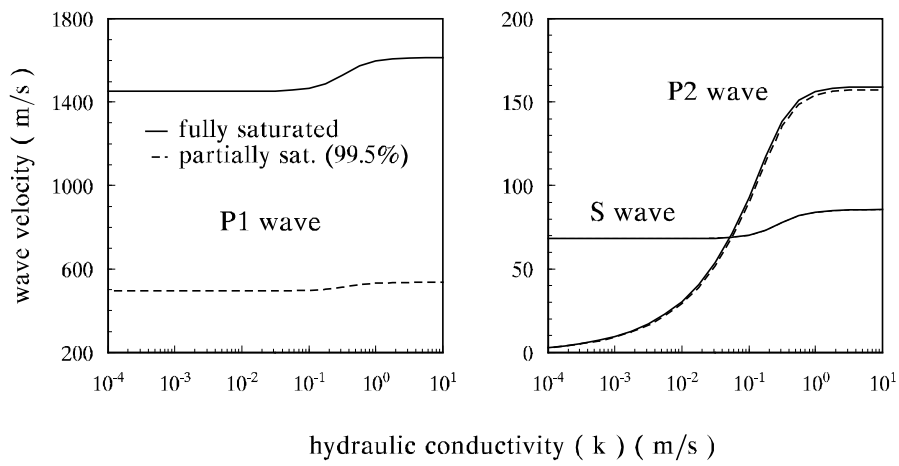
Figure 6. Wave propagation velocity amplitudes in the sediment vs. permeability.
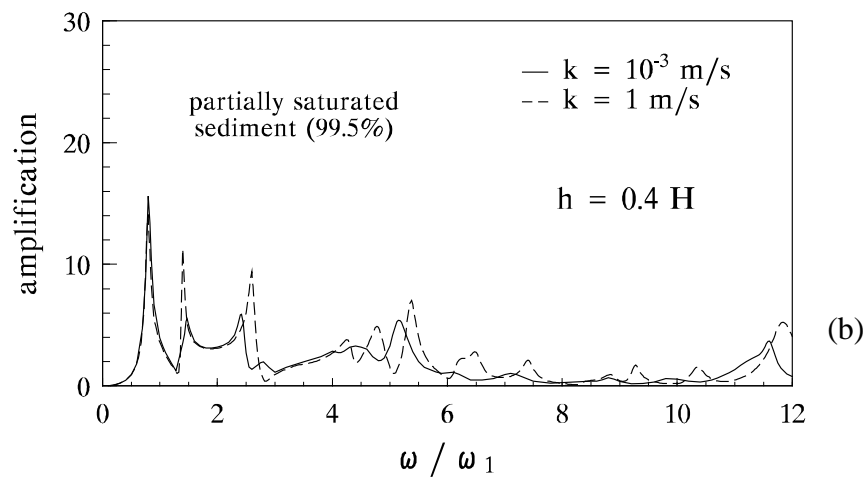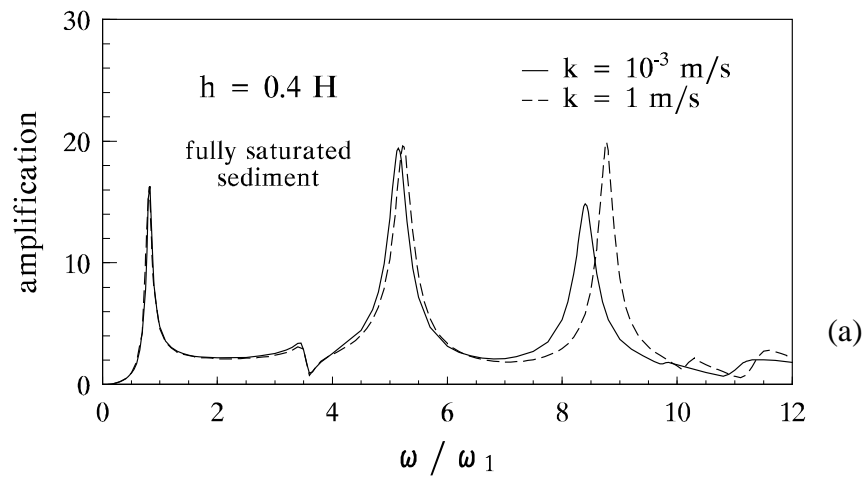
Figure 7a, b. Influence of sediment permeability. Horizontal amplification at the wall top to horizontal excitation for sediment thickness h/H = 0.4.

Figure 8a,b,c,d. Influence of sediment permeability. Local response of sediment to vertical excitation: vertical displacement of solid skeleton and hydrodynamic pressure for different points at water-sediment interface. d = distance from the wall face.
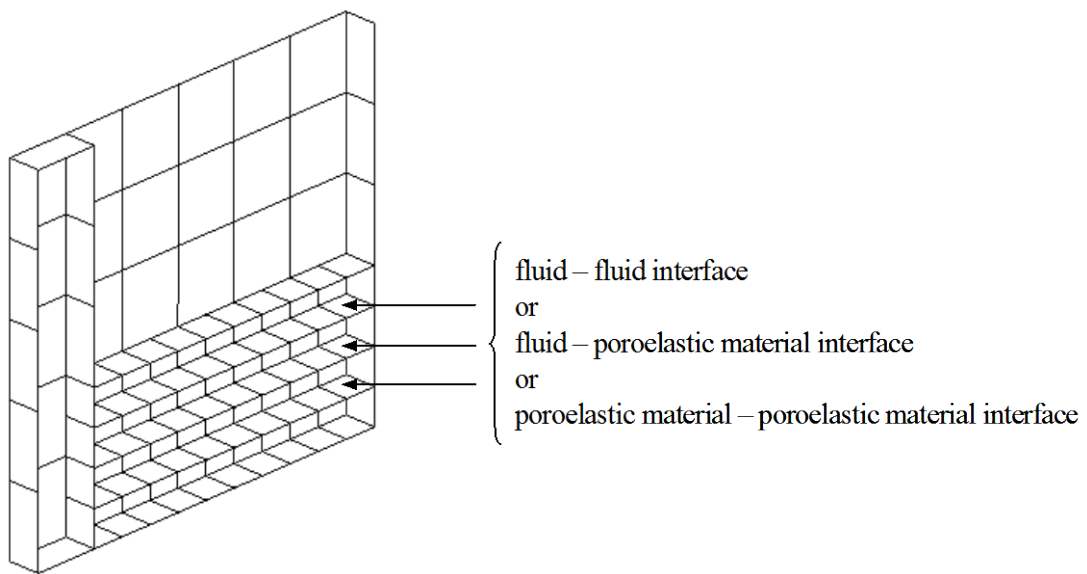
Figure 9. Heterogeneous sediment. Boundary Element discretization. See Table 1 for interface conditions.
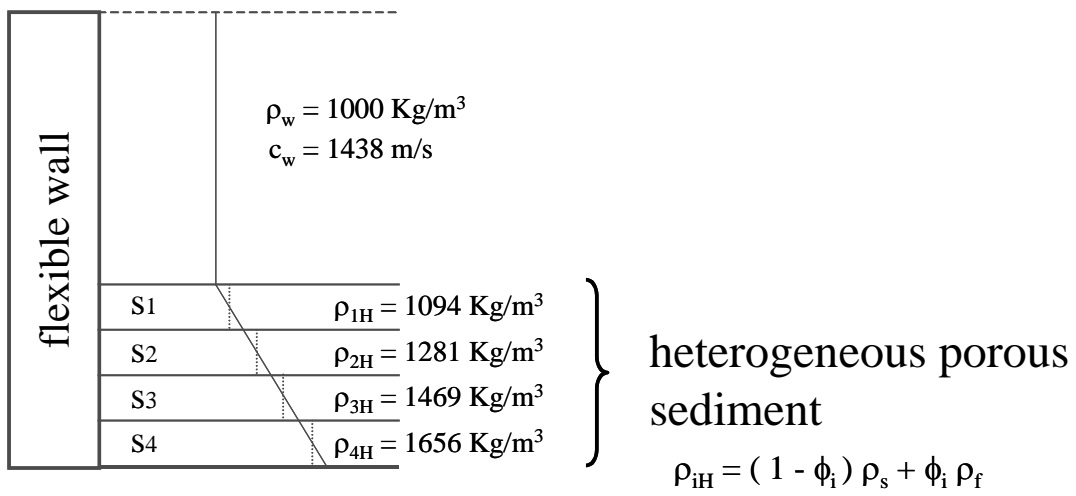
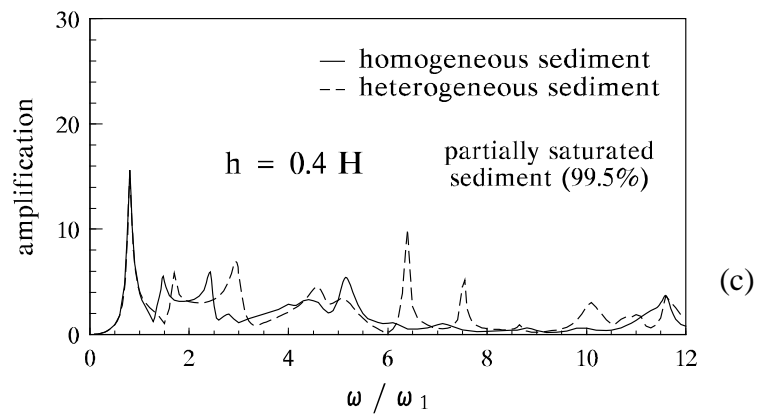Figure 10. Heterogeneous porous sediment stratum. See Table 2 for mechanical properties for three different saturation degrees.
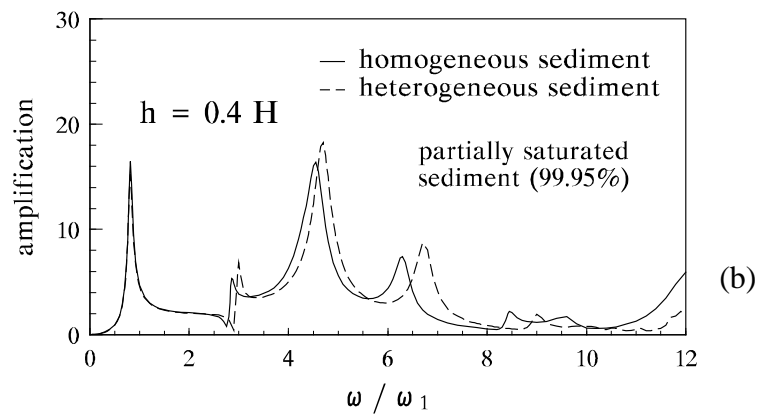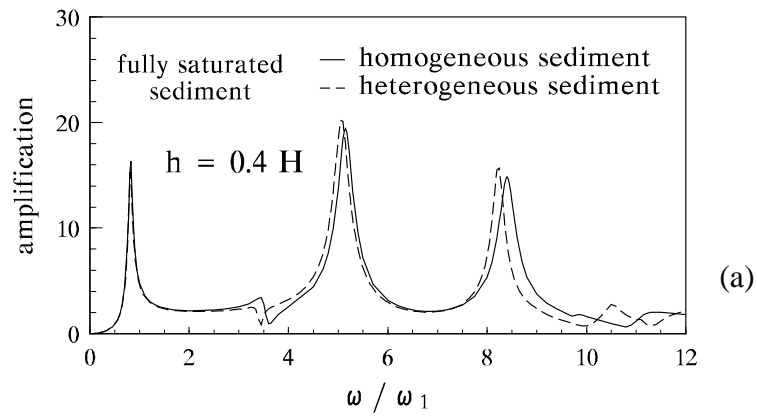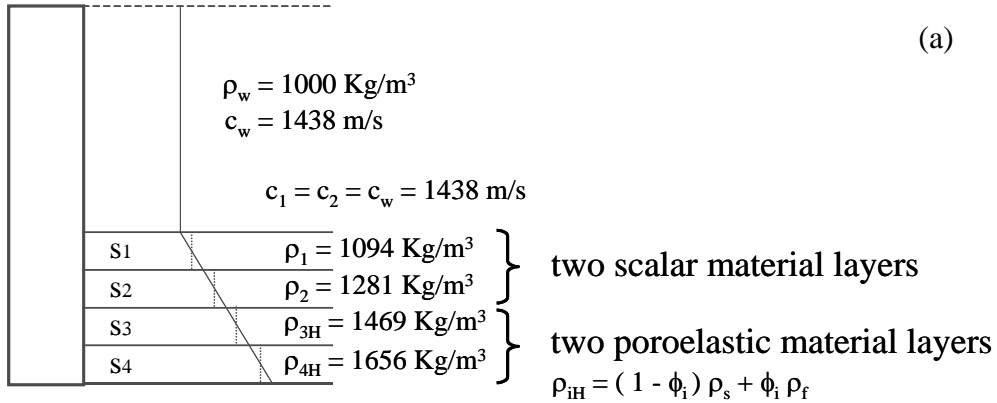
Figure 11a, b, c. Influence of sediment heterogeneity. Horizontal amplification at the wall top to horizontal excitation for sediment thickness h/H = 0.4.

partially consolidated

(a)

$\rho_w = 1000 \text{ Kg/m}^3$
$c_w = 1438 \text{ m/s}$

$c_1 = c_2 = c_w = 1438 \text{ m/s}$

S1	$\rho_1 = 1094 \text{ Kg/m}^3$
S2	$\rho_2 = 1281 \text{ Kg/m}^3$

two scalar material layers

S3	$\rho_{3H} = 1469 \text{ Kg/m}^3$
S4	$\rho_{4H} = 1656 \text{ Kg/m}^3$

two poroelastic material layers
$\rho_{iH} = (1 - \phi_i) \rho_s + \phi_i \rho_f$

non-consolidated

(b)

$\rho_w = 1000 \text{ Kg/m}^3$
$c_w = 1438 \text{ m/s}$

S1	$\rho_1 = 1094 \text{ Kg/m}^3$
S2	$\rho_2 = 1281 \text{ Kg/m}^3$
S3	$\rho_3 = 1469 \text{ Kg/m}^3$
S4	$\rho_4 = 1656 \text{ Kg/m}^3$

four scalar material layers

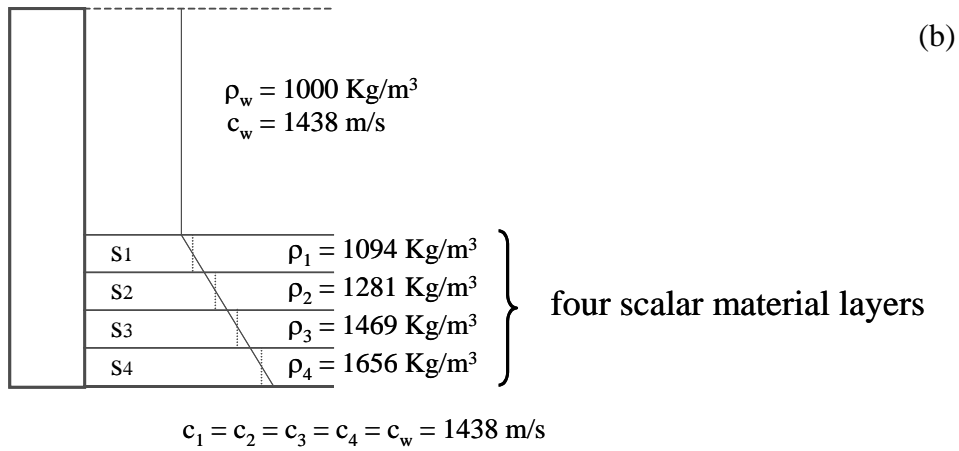$c_1 = c_2 = c_3 = c_4 = c_w = 1438 \text{ m/s}$

Figure 12a, b. Heterogeneous sediment stratum. (a): partially consolidated sediment; (b): non-consolidated sediment. See mechanical properties for poroelastic material layers in Table 3.
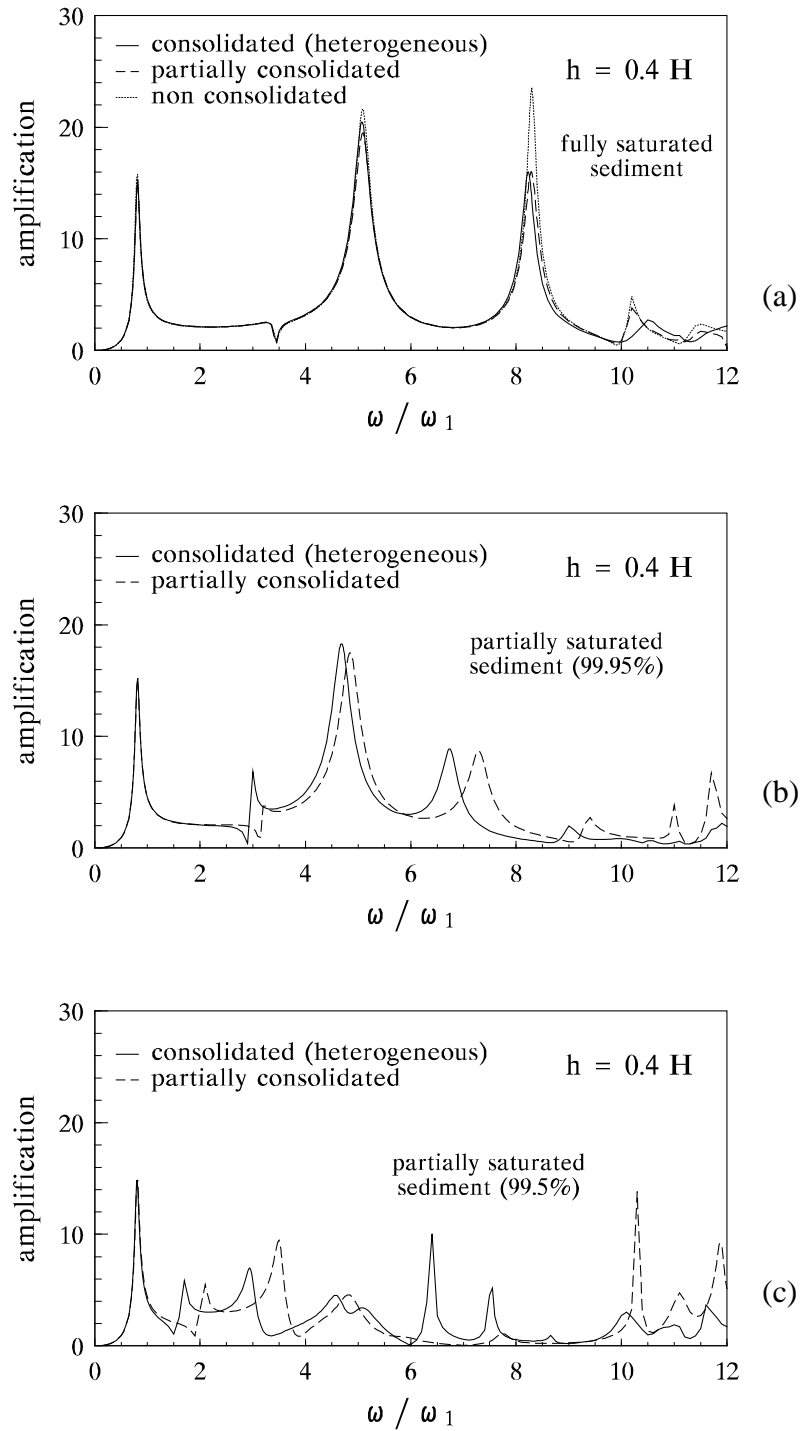
Figure 13a, b, c. Influence of consolidation degree. Fully and partially saturated sediments. Horizontal amplification at the wall top to horizontal excitation for sediment thickness h/H=0.4.
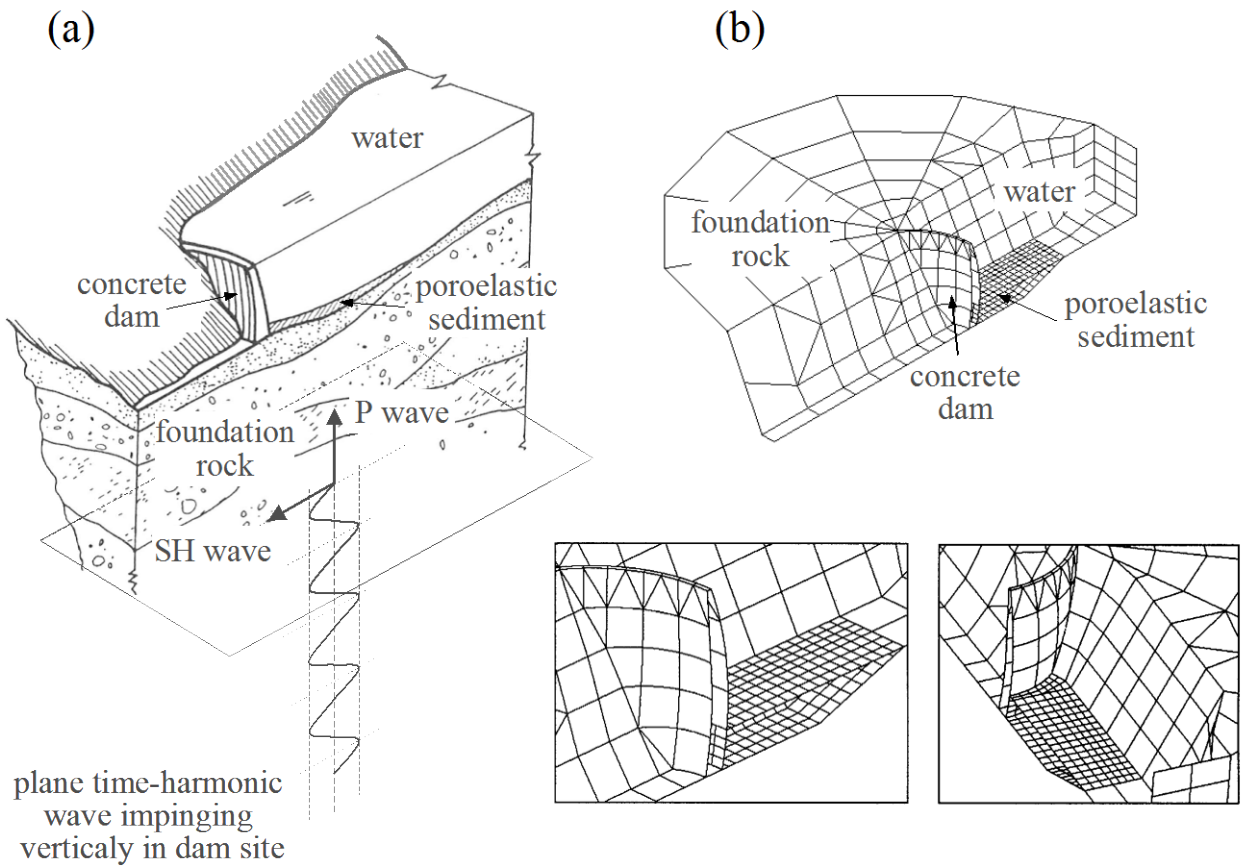
(a)

water

concrete dam

poroelastic sediment

P wave

foundation rock

SH wave

plane time-harmonic wave impinging verticaly in dam site

(b)

foundation rock

water

poroelastic sediment

concrete dam

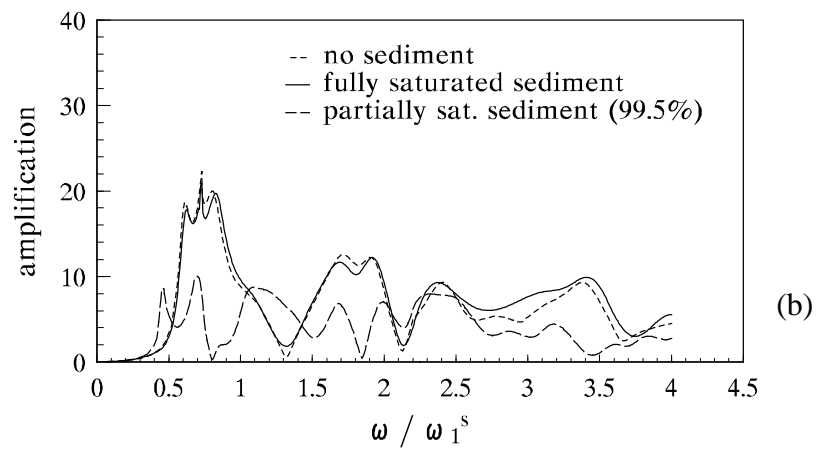Figure 14a, b. 3-D coupled problem. Seismic response of arch dams. BE model for the coupled system.
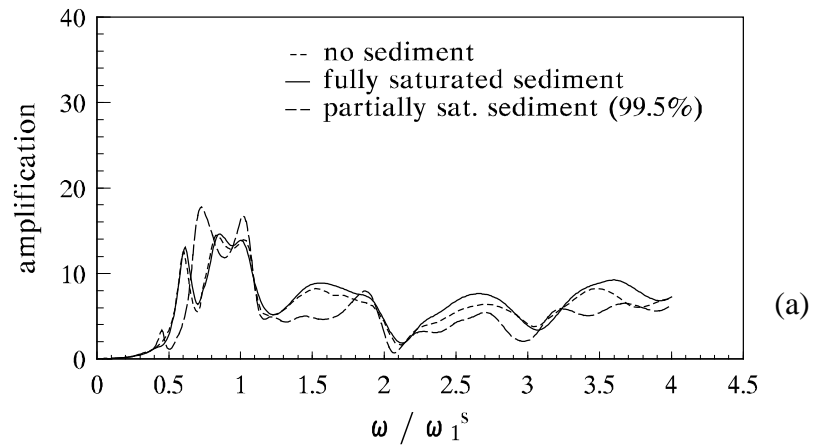
Figure 15a, b. 3-D Dynamic response of arch dams. Influence of sediments saturation degree. Upstream response at dam crest to ground motion: (a) upstream excitation (S wave); (b) vertical excitation (P wave).